

Energy stable neural network for gradient flow equations

Ganghua Fan^a, Tianyu Jin^a, Yuan Lan^a, Yang Xiang^{*a,b}, and Luchan Zhang^{†c}

^a*Department of Mathematics, The Hong Kong University of Science and Technology, Clear Water Bay, Hong Kong Special Administrative Region of China*

^b*Algorithms of Machine Learning and Autonomous Driving Research Lab, HKUST Shenzhen-Hong Kong Collaborative Innovation Research Institute, Futian, Shenzhen, China*

^c*College of Mathematics and Statistics, Shenzhen University, Shenzhen 518060, China*

September 20, 2023

Abstract

In this paper, we propose an energy stable network (EStable-Net) for solving gradient flow equations. The solution update scheme in our neural network EStable-Net is inspired by a proposed auxiliary variable based equivalent form of the gradient flow equation. EStable-Net enables decreasing of a discrete energy along the neural network, which is consistent with the property in the evolution process of the gradient flow equation. The architecture of the neural network EStable-Net consists of a few energy decay blocks, and the output of each block can be interpreted as an intermediate state of the evolution process of the gradient flow equation. This design provides a stable, efficient and interpretable network structure. Numerical experimental results demonstrate that our network is able to generate high accuracy and stable predictions.

Keywords— Deep learning, neural network architecture, energy stable, gradient flow equations

*Corresponding author. E-mail address: maxiang@ust.hk (Y.Xiang).

†Corresponding author. E-mail address: zhanglc@szu.edu.cn (L.Zhang).

1 Introduction

Partial differential equations are important tools in solving a wide range of problems in science and engineering fields. Over the past twenty years, deep neural networks (DNNs) [12, 19] have demonstrated their power in science and engineering applications, and efforts have been made to employ DNNs to solve complex partial differential equations as an alternative to the traditional numerical schemes, especially for problems in high dimensions.

Early works [5, 17] use feedforward neural network to learn the initial/boundary value problem by constraining neural networks using differential equation. Methods using continuous dynamical systems to model high-dimensional nonlinear functions used in machine learning were proposed in [6]. A deep learning-based approach to solve high dimensional parabolic partial differential equations (PDEs) based on the formulation of stochastic differential equations was developed in [14]. Benefiting from autograd differentiation, physics-informed neural network (PINN) [25] was derived for a wide variety of PDEs, using information of the PDE with initial/boundary conditions and a few time-space points randomly sampled in the solution domain to approximate the solution and trained by minimizing the mean squared error loss of the PDE. The Deep Ritz Method [7] was proposed based on representing the trial functions by deep neural networks, which is in the variational form with the total energy as the loss. The Deep Galerkin method (DGM) was proposed in [29] with the PDE as the loss for the neural network approximation of the solution. The Weak Adversarial Network (WAN) [35] solves a PDE by a generative adversarial network using the weak form of the PDE as the loss. In [23], a deep mixed residual method (MIM) is proposed to solve high order PDEs by rewriting the original equation into a first-order system and taking the first-order system's residual as the loss function. The random feature method (RFM) was proposed in [2] for solving PDEs where the neural network is utilized to learn random feature functions and the residual of PDE is used as the loss function. The Friedrichs learning [1] employs Friedrichs minimax formulation as the loss to approximate solution of PDEs. In these methods, neural networks are trained for individual PDE problems, i.e., for different PDE problems, different neural networks need to be trained.

Another class of approaches employ neural networks to learn the operators. The Fourier Neural Operator (FNO) was developed in [20], which focuses on mappings

between infinite-dimensional function spaces by using Fourier Transform to approximate the linear or nonlinear operators. The Deep Operator Network (DeepONet) proposed in [22] learns nonlinear operators associated with PDEs from data based on the approximation theorem for operators by neural networks. In [15], parametric PDE problems with artificial neural networks were solved by expressing the physical quantity interested as a function of random coefficient. A compact network architecture to solve electrical impedance tomography problem based on the numerically low-rank property of the forward and inverse maps was proposed in [10]. There are methods based on learning Green's functions for solving PDEs [11, 36]. A neural network to approximate functionals without curse of dimensionality based on the method of Barron space was developed in [34]. Multigrid networks for solving parameterized partial differential equations were proposed in [4]. In [21], the DeepPropNet was developed to approximate the evolution operator over a long time by using a single neural network propagator recursively. Based on the operator splitting method, [18] proposed the Deep Operator-Splitting Network (DOSnet) for solving evolution equations. This network takes the form of block structure and each block models the transition between the states in the physical evolution systems rather than mapping the input into some higher dimensional features, and the properties of the PDE is reflected in the network by using the nonlinear part of the operator as the activation function.

A class of widely used mathematical models take the form of gradient flows to minimize some total energy, for which many numerical methods have been developed to preserve the energy dissipation property [3, 8, 9, 13, 24, 26–28, 30–33, 37]. In this paper, we propose an energy stable neural network (EStable-Net) to solve the gradient flow equations. Based on the block architecture Autoflow of the DOSNet [18], we introduce an auxiliary variable and encoded it into the blocks to enforce the energy decay property along the network, which is consistent with the physical property of the gradient flow. This design provides a stable, efficient and interpretable network structure. Experiments on several partial differential equations demonstrate that our network is able to generate high accuracy and stable predictions.

The rest of this paper is organized as follows. In Section 2, we introduce the auxiliary variable of gradient flow equation, and reformulate the original equation into a new equivalent system. In Section 3, we present our energy stable neural network EStable-Net inspired by the auxiliary variable based equivalent form of the gradient flow equation presented in Section 2. We prove that a discrete energy of each block in the network is decreasing along the network. In section 4, We present some numerical

experiments using our EStable-Net. We conclude this paper in Section 5.

2 Gradient flow equations

In this section, we first briefly review the gradient flow equation and its energy dissipation property. We then introduce the auxiliary variable of the gradient flow equation, and reformulate the original equation into a new equivalent system, which suggests the neural network to be presented in the next section.

2.1 Gradient flow equations and energy dissipation property

The general form of gradient flow equations is:

$$\phi_t = -\mathcal{G}(\mathcal{D}\phi + f(\phi)), \quad (x, t) \in \Omega \times [0, T] \quad (1)$$

$$\phi(0, x) = \phi_0(x), \quad x \in \Omega. \quad (2)$$

where \mathcal{G} and \mathcal{D} are positive operators. The boundary conditions can be the periodic boundary conditions or homogeneous Neumann boundary conditions for simplicity.

By specifying operators \mathcal{G} and \mathcal{D} , we have some commonly used gradient flow equations:

- The Allen-Cahn equation, $\mathcal{G} = 1, \mathcal{D} = -\epsilon^2\Delta, f(\phi) = \phi^3 - \phi$, where ϵ is the interfacial width, that is

$$\phi_t = \epsilon^2\Delta\phi - \phi^3 + \phi.$$

- The Cahn-Hilliard equation, $\mathcal{G} = -\Delta, \mathcal{D} = -\epsilon^2\Delta, f(\phi) = \phi^3 - \phi$, where ϵ is the interfacial width, that is

$$\phi_t = \Delta(-\epsilon^2\Delta\phi + \phi^3 - \phi).$$

The energy of the gradient flow equation (1) is

$$E(\phi) = \int_{\Omega} \left(\frac{1}{2} |\mathcal{D}^{1/2}\phi|^2 + F(\phi) \right) dx, \quad (3)$$

where $\mathcal{D}^{1/2}(\mathcal{D}^{1/2})^* = (\mathcal{D}^{1/2})^*\mathcal{D}^{1/2} = \mathcal{D}$, and the variational derivative of $\int_{\Omega} F(\phi)dx$ is $f(\phi)$ in (1). Notice that the energy (3) dissipates along equation (1) by taking the inner product of (1) with $\mathcal{D}\phi + f(\phi)$:

$$(\phi_t, \mathcal{D}\phi + f(\phi)) = (-\mathcal{G}(\mathcal{D}\phi + f(\phi)), \mathcal{D}\phi + f(\phi)) = -\|\mathcal{G}^{1/2}(\mathcal{D}\phi + f(\phi))\|^2. \quad (4)$$

Hence,

$$\frac{d}{dt}E(\phi(t)) = \left(\frac{\delta E}{\delta \phi}, \phi_t \right) = (\mathcal{D}\phi + f(\phi), \phi_t) = -\|\mathcal{G}^{1/2}(\mathcal{D}\phi + f(\phi))\|^2 \leq 0. \quad (5)$$

Here $\mathcal{G}^{1/2}(\mathcal{G}^{1/2})^* = (\mathcal{G}^{1/2})^*\mathcal{G}^{1/2} = \mathcal{G}$.

2.2 Auxiliary variable and equivalence system

We introduce a auxiliary variable U to be

$$U = \sqrt{\frac{1}{2}|\mathcal{G}^{-1/2}\phi|^2 + \frac{1}{2}|\mathcal{D}^{1/2}\phi|^2 + F(\phi) + C}, \quad (6)$$

where $\mathcal{G}^{-1/2}$, C is a constant to maintain non-negativity of the function underneath the square root.

The original energy (3) can be reformulated as

$$\tilde{E}(\phi, U) = \int_{\Omega} \left(-\frac{1}{2}|\mathcal{G}^{-1/2}\phi|^2 + U^2 - C \right) dx. \quad (7)$$

Note that the new energy (7) is equivalent to the original energy (3). Compared with the original energy, the quadratic term of the auxiliary variable U in the new energy introduces a term $\frac{1}{2}|\mathcal{G}^{-1/2}\phi|^2$ and a negative term is added at the outside. This kind of numerical treatment of adding one term first and subtracting it afterwards has been used in convex splitting schemes, e.g. [3, 9, 30], with the purpose of constructing stable and linear numerical schemes.

The new system with auxiliary variable U is

$$\phi_t = \phi - \mathcal{G}(H_1(\phi)U), \quad (8)$$

$$U_t = \frac{1}{2}H_2(\phi)\phi_t, \quad (9)$$

$$H_1(\phi) = \frac{\mathcal{G}^{-1}\phi + \mathcal{D}\phi + f(\phi)}{\sqrt{\frac{1}{2}|\mathcal{G}^{-1/2}\phi|^2 + \frac{1}{2}|\mathcal{D}^{1/2}\phi|^2 + F(\phi) + C}}, \quad (10)$$

$$H_2(\phi) = \frac{\mathcal{G}^{-1/2}\phi\mathcal{G}^{-1/2} + \mathcal{D}^{1/2}\phi\mathcal{D}^{1/2} + f(\phi)}{\sqrt{\frac{1}{2}|\mathcal{G}^{-1/2}\phi|^2 + \frac{1}{2}|\mathcal{D}^{1/2}\phi|^2 + F(\phi) + C}}, \quad (11)$$

$$\phi(0, x) = \phi_0(x), \quad (12)$$

$$U(0, x) = \sqrt{\frac{1}{2}|\mathcal{G}^{-1/2}\phi_0|^2 + \frac{1}{2}|\mathcal{D}^{1/2}\phi_0|^2 + F(\phi_0) + C}. \quad (13)$$

It is easy to see that the new system (8)-(13) is equivalent to the original gradient flow system (1)-(2). Besides, the modified energy (7) satisfies dissipative law along the equivalent system:

$$\begin{aligned} \frac{d}{dt}\tilde{E}(\phi(t), U(t)) &= \left(\frac{\delta\tilde{E}}{\delta\phi}, \phi_t\right) + \left(\frac{\delta\tilde{E}}{\delta U}, U_t\right) \\ &= (-\mathcal{G}^{-1}\phi, \phi_t) + (2U, U_t) \\ &= (-\mathcal{G}^{-1}\phi, \phi_t) + (U, H_2(\phi)\phi_t) \\ &= (\phi_t, -\mathcal{G}^{-1}\phi + H_2(\phi)U) \\ &= (\phi_t, -\mathcal{G}^{-1}\phi + H_1(\phi)U) \\ &= (\phi_t, -\mathcal{G}^{-1}\phi_t) \\ &= -\|\mathcal{G}^{-1/2}\phi_t\|^2 \leq 0. \end{aligned} \quad (14)$$

Here, the third equality is obtained by using (9), the fifth equality is easy to see from the form of (10)-(11), and equation (8) is used to obtain the sixth equality.

The idea of introducing auxiliary variable and reformulating the original system into an equivalent system has been used in [24, 32], where the purpose of the variable substitution is to reformulate the nonlinear terms in the free energy into quadratic form, leading to a linear numerical scheme and in the meantime, maintaining the energy dissipation property.

Here, we follow the same approach but add a new term based on the specific operator of the gradient flow equation as shown in (7), and rewrite all the other free

energy terms into a quadratic part. The propose of this treatment is to generate a structure that is learning-friendly for neural network while preserving the energy decay property (to be presented in the next section).

Remark 1. *The construction of the auxiliary variable U is not unique. In this problem, since the energy density is bounded below, we can take the entire energy density to construct the the auxiliary variable, that is*

$$\tilde{U} = \sqrt{\frac{1}{2}|\mathcal{D}^{1/2}\phi|^2 + F(\phi) + \tilde{C}}, \quad (15)$$

where \tilde{C} is a constant to maintain non-negativity of the function underneath the square root. The new evolution system reads as

$$\phi_t = -\mathcal{G}(\tilde{H}_1(\phi)\tilde{U}), \quad (16)$$

$$\tilde{U}_t = \frac{1}{2}\tilde{H}_2\phi_t, \quad (17)$$

$$\tilde{H}_1(\phi) = \frac{\mathcal{D}\phi + f(\phi)}{\sqrt{\frac{1}{2}|\mathcal{D}^{1/2}\phi|^2 + F(\phi) + \tilde{C}}}, \quad (18)$$

$$\tilde{H}_2(\phi) = \frac{1}{2} \frac{\mathcal{D}^{1/2}\phi\mathcal{D}^{1/2} + f(\phi)}{\sqrt{\frac{1}{2}|\mathcal{D}^{1/2}\phi|^2 + F(\phi) + \tilde{C}}}. \quad (19)$$

It can be easily checked that this new system also preserve the energy decay property with respect to the new energy

$$E_{new}(\phi, \tilde{U}) = \int_{\Omega} (\tilde{U}^2 - \tilde{C}) \, dx, \quad (20)$$

that is

$$\frac{dE_{new}}{dt} = (2\tilde{U}, \frac{1}{2}\tilde{H}_2\phi_t) = (\tilde{H}_2\tilde{U}, \phi_t) = (-\mathcal{G}^{-1}\phi_t, \phi_t) = -\|\mathcal{G}^{-1/2}\phi_t\|^2 \leq 0. \quad (21)$$

3 Energy stable neural network

In this section, we present our energy stable neural network EStable-Net inspired by numerical discretization of the auxiliary variable based form (8) and (9) of the gradient flow equation given in the previous section.

3.1 Energy stable network structure

The architecture of our energy stable neural network EStable-Net for solving gradient flow equations consists of a few energy decay blocks, with input being the initial condition ϕ^0 and the output the solution ϕ^T at time T . The output of the n -th block are quantities ϕ^n and U^n , which have the same dimensions as the discretized solution ϕ and the discretized auxiliary variable U , respectively, and such output can be interpreted as an intermediate state of the evolution process of the gradient flow equation. This block architecture follows the Autoflow structure in the neural network DOSnet [18] for solving evolution equations.

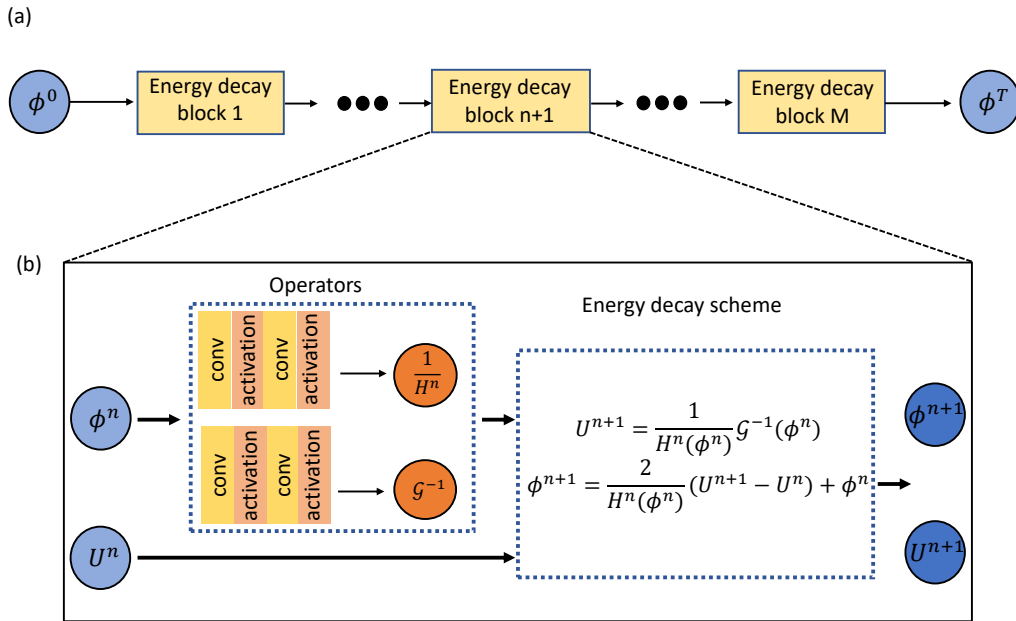


Figure 1: Network architecture of EStable-Net. (a) The overall Autoflow structure of the network. (b) The structure within each energy decay block. Here M is the number of blocks in the network.

Inside the $(n+1)$ -th block, the pair (ϕ^n, U^n) are updated to (ϕ^{n+1}, U^{n+1}) following the formulation

$$U^{n+1} = \frac{1}{H^n(\phi^n)} \mathcal{G}^{-1}(\phi^n), \quad (22)$$

$$\phi^{n+1} = \frac{2}{H^n(\phi^n)} (U^{n+1} - U^n) + \phi^n. \quad (23)$$

We learn the operators $\frac{1}{H^n}$ and \mathcal{G}^{-1} by using a few convolution layers with activations. The above update formulation enables a decreasing property for a discretized version of the total energy of the gradient flow equation (Eq. (26) below); see the proof in the next subsection. The architecture of this proposed neural network EStable-Net is illustrated in Figure 1.

This network structure is inspired by the following discrete scheme associated with the continuum energy stable formula (8)-(9) for the gradient flow equation (1)-(2):

$$\phi^n = \mathcal{G} (H^n(\phi^n)U^{n+1}), \quad (24)$$

$$U^{n+1} - U^n = \frac{1}{2}H^n(\phi^n)(\phi^{n+1} - \phi^n), \quad (25)$$

for some function $H^n(\cdot)$. Note that this scheme is not necessary an accurate approximation of the gradient flow equation (8)-(9). Instead, it provides a simple form that enables decreasing of the energy for the discretized evolution given by Eqs. (22)-(23) or (24)-(25), which is defined as

$$\tilde{E}(\phi^n, U^n) = -\frac{1}{2}\|\mathcal{G}^{-1/2}\phi^n\|^2 + \|U^n\|^2 - C|\Omega|. \quad (26)$$

This energy is the discrete counterpart of the continuum energy in Eq. (7). It can be proved that this discrete energy is indeed decreasing following the discretized evolution given by Eqs. (22)-(23) or (24)-(25); see the proof in the next subsection. This energy decay property is consistent with the physical property of the gradient flow. Combined with the block network structure, i.e., Autoflow [18], that mimics the exact evolution flow, our EStable-Net is an efficient neural network that has the advantages of easy to train, and being able to provide accurate and stable predictions, as will be seen in the numerical examples presented in the next section.

Using training data (ϕ^0, ϕ^T) , e.g., generated by some high-precision classical numerical method, the learnable parameters $\boldsymbol{\theta} = \{\theta_j\}_{j=1}^M$ inside energy decay network can be obtained via minimizing the mean square error loss (MSE):

$$\boldsymbol{\theta}^* = \arg \min_{\boldsymbol{\theta}} \mathcal{L}(\boldsymbol{\theta}) = \frac{1}{N} \sum_{i=1}^N \|\mathcal{N}_{\boldsymbol{\theta}}(\phi^{(i)}(x, 0)) - \phi^{(i)}(x, T)\|^2, \quad (27)$$

where N is number of the training data, symbols with superscript i represents the i -th sample, \mathcal{N} denotes the neural network EStable-Net, $\mathcal{N}_{\boldsymbol{\theta}}(\phi^{(i)}(x, 0))$ is i -th neural network output and $\phi^{(i)}(x, T)$ is the ground truth, and $\|\cdot\|$ is the L^2 norm.

If \mathcal{G} is not the identity operator, we can make the network easier to train by adding the following contribution to the loss in Eq. (27):

$$\beta \sum_{n=1}^M \frac{1}{N} \sum_{i=1}^N \|\phi^{n,(i)} + \mathcal{G}(H^n(\phi^{n,(i)})U^{n+1,(i)})\|^2, \quad (28)$$

where $\beta > 0$ is some factor. Here the differential operator \mathcal{G} can be calculated using autograd. The effect of this contribution in the loss is to make sure that the operator \mathcal{G}^{-1} in Eq. (22) can be learned more accurately in the training process.

Note that the discrete energy of the gradient flow equation is

$$E^n = \frac{1}{2} \|\mathcal{D}^{1/2} \phi^n\|^2 + \int_{\Omega} F(\phi^n) dx, \quad (29)$$

which is in different from the discrete energy defined in (26) along the neural network EStable-Net, because along the network U^n is updated following Eq. (22), which is not necessarily equal to exact value of the auxiliary variable U defined in Eq. (6). However, benefited from the ground truth constraints of the supervised learning, we also observe dissipation of the original discrete energy in the numerical experiments; see next section.

Remark 2. Here we present another neural network formula with energy decay property based on the alternative auxiliary variable \tilde{U} defined in Eq. (15) in Remark 1 in Section 2.2. This alternative neural network formulation applies to the case of the operator \mathcal{G} is the identity operator, e.g. the Allen-Cahn equation.

Based on this auxiliary variable and the associated evolution equations (16) and (17), when \mathcal{G} is the identity operator, we consider the following simplified evolution system to develop the neural network:

$$\phi_t = -H(\phi, t)\tilde{U}, \quad (30)$$

$$\tilde{U}_t = \frac{1}{2}H(\phi, t)\phi_t, \quad (31)$$

where $H(\phi, t)$ is some function.

A time discretization scheme for the above evolution system is

$$\frac{\phi^{n+1} - \phi^n}{\Delta t} = -H^n(\phi^n)\tilde{U}^{n+1}, \quad (32)$$

$$\frac{\tilde{U}^{n+1} - \tilde{U}^n}{\Delta t} = \frac{1}{2}H^n(\phi^n)\frac{\phi^{n+1} - \phi^n}{\Delta t}, \quad (33)$$

where Δt is the time step size and is chosen as $\Delta t = T/M$ in the neural network.

The neural network formulation corresponding to this alternative auxiliary variable \tilde{U} in (15) is

$$\phi^{n+1} = \phi^n - \frac{\Delta t H^n(\phi^n)}{1 + \frac{1}{2} \Delta t H^n(\phi^n)^2} \tilde{U}^n, \quad (34)$$

$$\tilde{U}^{n+1} = \frac{1}{1 + \frac{1}{2} \Delta t H^n(\phi^n)^2} \tilde{U}^n. \quad (35)$$

In this alternative neural network formulation, the operator $H^n(\cdot)$ is learned in the $(n+1)$ -th block in the neural network presented in Subsection 3.1.

The energy for the discrete evolution scheme in Eq. (34)-(35), corresponding to the continuum energy in Eq. (20), is defined as

$$\tilde{E}_{new}(\phi^n, \tilde{U}^n) = \|\tilde{U}^n\|^2 - \tilde{C}|\Omega|. \quad (36)$$

It is obvious from Eq. (35) that

$$\tilde{E}_{new}(\phi^{n+1}, \tilde{U}^{n+1}) \leq \tilde{E}_{new}(\phi^n, \tilde{U}^n), \quad \text{for } n \geq 0. \quad (37)$$

That is, the energy $\tilde{E}_{new}(\phi^n, \tilde{U}^n)$ is decreasing along the neural network.

3.2 Proof of the energy decay property of EStable-Net

In this subsection, we prove that following Eqs. (22)-(23), or equivalently (24)-(25), the discrete energy (26) is decreasing, i.e.,

$$\tilde{E}(\phi^{n+1}, U^{n+1}) \leq \tilde{E}(\phi^n, U^n), \quad \text{for } n \geq 0. \quad (38)$$

Taking inner product of $-\mathcal{G}^{-1}(\phi^{n+1} - \phi^n)$ with (24), we obtain

$$-(\phi^{n+1} - \phi^n, \mathcal{G}^{-1}(\phi^{n+1} - \phi^n)) = -(\phi^{n+1} - \mathcal{G}(H^n(\phi^n)U^{n+1}), \mathcal{G}^{-1}(\phi^{n+1} - \phi^n)).$$

That is,

$$\begin{aligned} -\|\mathcal{G}^{-1/2}\phi^{n+1} - \mathcal{G}^{-1/2}\phi^n\|^2 &= ((H^n(\phi^n)U^{n+1}, \phi^{n+1} - \phi^n) - \frac{1}{2}\|\mathcal{G}^{-1/2}\phi^{n+1}\|^2 \\ &\quad + \frac{1}{2}\|\mathcal{G}^{-1/2}\phi^n\|^2 - \frac{1}{2}\|\mathcal{G}^{-1/2}\phi^{n+1} - \mathcal{G}^{-1/2}\phi^n\|^2). \end{aligned} \quad (39)$$

Taking inner product of $2U^{n+1}$ with (25), we have

$$2(U^{n+1} - U^n, U^{n+1}) = (H^n(\phi^n)(\phi^{n+1} - \phi^n), U^{n+1}).$$

That is,

$$\|U^{n+1}\|^2 - \|U^n\|^2 + \|U^{n+1} - U^n\|^2 = (H^n(\phi^n)(\phi^{n+1} - \phi^n), U^{n+1}). \quad (40)$$

From (39) and (40), we can express the discrete energy difference as

$$\begin{aligned} \tilde{E}(\phi^{n+1}, U^{n+1}) - \tilde{E}(\phi^n, U^n) &= -\frac{1}{2}\|\mathcal{G}^{-1/2}\phi^{n+1}\|^2 + \frac{1}{2}\|\mathcal{G}^{-1/2}\phi^n\|^2 + \|U^{n+1}\|^2 - \|U^n\|^2, \\ &= -\frac{1}{2}\|\mathcal{G}^{-1/2}\phi^{n+1} - \mathcal{G}^{-1/2}\phi^n\|^2 - ((H^n(\phi^n)U^{n+1}, \phi^{n+1} - \phi^n) \\ &\quad - \|U^{n+1} - U^n\|^2 + (H^n(\phi^n)(\phi^{n+1} - \phi^n), U^{n+1}), \\ &= -\frac{1}{2}\|\mathcal{G}^{-1/2}\phi^{n+1} - \mathcal{G}^{-1/2}\phi^n\|^2 - \|U^{n+1} - U^n\|^2 \leq 0. \end{aligned} \quad (41)$$

This proves that the discrete energy defined in Eq. (26) is indeed decreasing along our neural network EStable-Net.

4 Numerical experiments

In this section, we perform numerical experiments of the EStable-Net on classical gradient flow equations. We focus on the Allen-Cahn equation:

$$\phi_t = \epsilon^2 \Delta \phi - \phi^3 + \phi, \quad x \in \Omega, \quad (42)$$

$$\phi_0 = \phi(x, 0), \quad x \in \Omega, \quad (43)$$

with periodic boundary conditions. The associated energy is

$$E(\phi) = \int_{\Omega} \left(\frac{\epsilon^2}{2} |\nabla \phi|^2 + \frac{1}{4} (\phi^2 - 1)^2 \right) dx. \quad (44)$$

The update scheme of our neural network EStable-Net in Eqs. (22) and (23) for the Allen-Cahn equation is

$$U^{n+1} = \frac{1}{H^n(\phi^n)} \phi^n, \quad (45)$$

$$\phi^{n+1} = \phi^n + \frac{2}{H^n(\phi^n)} (U^{n+1} - U^n), \quad (46)$$

where the operator $H^n(\cdot)$ is learned by this network.

4.1 Allen-Cahn equation in one dimension

In this subsection, we solve the Allen-Cahn equation in one dimension (1D). In this case, the spatial domain $\Omega = [-1, 1]$, and $\epsilon = 0.01$.

We choose $M = 4$ energy decay blocks in the network EStable-Net, and each block is composed of Conv1d-Tanh-Conv1d-Tanh, where Conv1d is a 1D convolution layer and Tanh is the activation using the tanh function. The activation function is not applied in the last layer for better accuracy. The number of channels is $1-16-1-16-1$ with kernel size 21. Under this setting, our EStable-Net has 5512 trainable parameters. We use xavier uniform initialization for weights and the batch size is 16. The optimizer of our model is Adam [16] with initial learning rate 10^{-3} and L^2 regularization weight decay rate 10^{-6} . The learning rate decays by half every 50 epochs, and restarts for each 200 epochs.

The inputs ϕ_0 are generated by combing fourier basis function with frequency less than 8 and coefficients sampled from normal distribution. We use 256 evenly spaced grid points to discretize the spacial domain $[-1, 1]$. The label data $\phi(x, T)$ at $T = 5$ is calculated by pseudo-spectral method with the Fast Fourier Transform. For the time discretization, we adopt ode45 solver in MATLAB. We generate 1120 pairs of data $\phi(x, 0)$ and $\phi(x, 5)$, and 784 of them are used for training while the left 336 are used for testing.

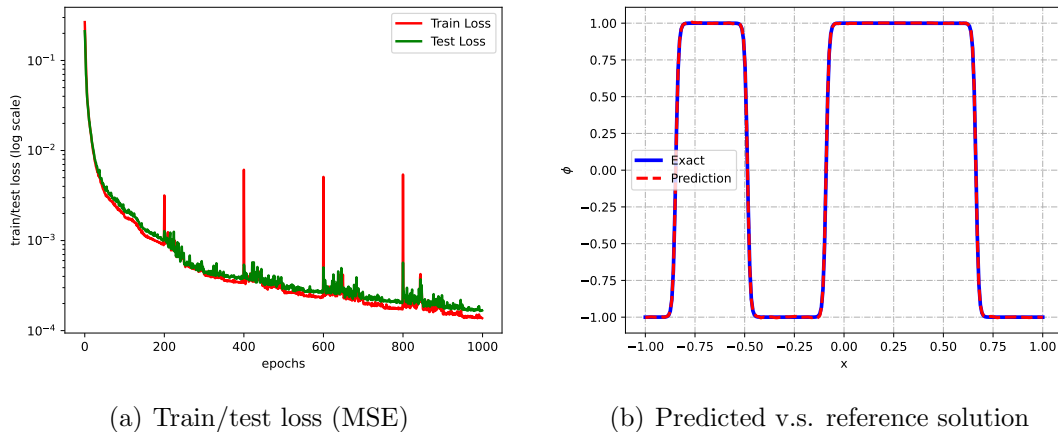
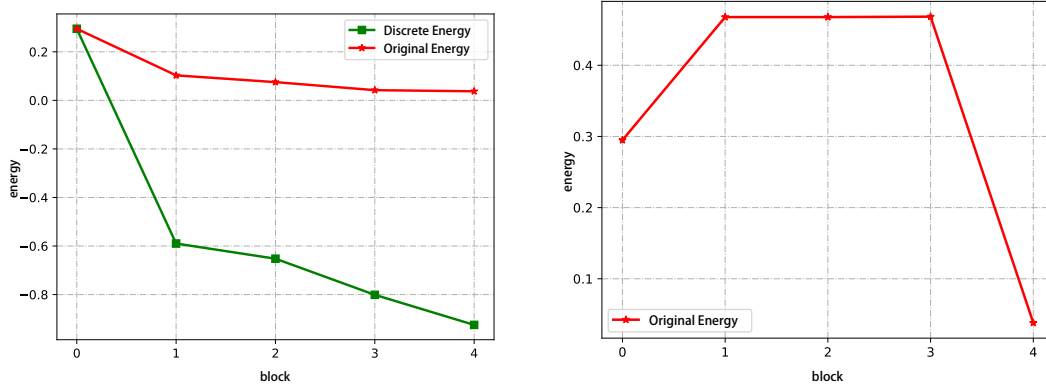


Figure 2: 1D Allen-Cahn equation: EStable-Net accuracy

Results of accuracy of EStable-Net on this 1D Allen Cahn equation are shown in Figure 2. After 1000 epochs of training, the test loss reaches about 1.6×10^{-4} and the

relative L^2 error reaches 7.8×10^{-3} . Figure 2(b) shows an example that the prediction of our network agrees well with the exact solution.



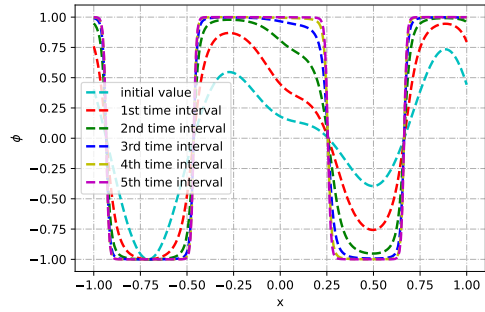
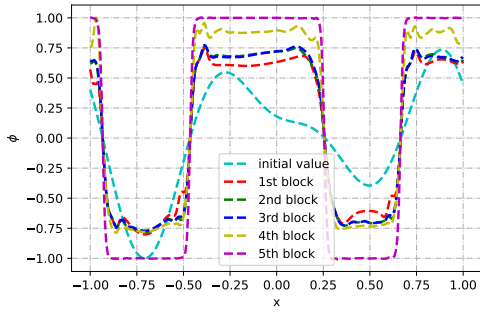
(a) Energies after each block in EStable-Net (b) Energy after each block in a plain network without the energy stable design

Figure 3: 1D Allen-Cahn equation: energy comparisons

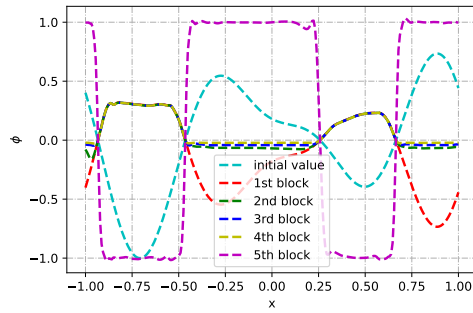
By randomly selecting 256 examples and passing them into the trained EStable-Net, we output the discrete energy in Eq. (26) after each block. We find that in all the samples, the discrete energy is decreasing block by block, as predicted by analysis. Moreover, we also find that the original energy in Eq. (3) is also decreasing block by block. These results of energies are shown in Figure 3(a).

The output of the intermediate and final blocks in EStable-Net and the corresponding snapshots in the evolution of the solution of the 1D Allen-Cahn equation with equal time increment $T/4$ obtained by numerical method are shown in Figure 4(a) and (b), respectively. It can be seen that the evolution trend of the output of the intermediate blocks in ECDnet is consistent with the evolution of the gradient flow equation. For example, within the interval $[-0.5, 0]$, the output of EStable-Net of the series of blocks is approaching the constant value 1, which is the same as the evolution of the solution of the 1D Allen-Cahn equation.

We also compare the evolving of the energy with that by using a "plain" network based on these selected samples; see Figure 3(b). The "plain" network does not have the auxiliary variable U and the associated energy stable property, and ϕ is learned following $\phi^{n+1} = H^n(\phi^n)$; other training settings and number of parameters are the same as EStable-Net. In this case, the energy is the original energy in Eq. (3). It can be seen that the energy increases first through the intermediate blocks and only



(a) Output after each block in EStable-Net (b) snapshots in the evolution of the 1D Allen-Cahn equation with time interval $T/4$



(c) Output after each block in the plain network

Figure 4: 1D Allen-Cahn equation: intermediate and final states comparisons

decreases at the last block, which is not consistent with the property of the gradient flow. The output of the intermediate and final blocks in this plain network are shown in Figure 4(c). It can be seen that the intermediate states given by this plain network are not consistent with the evolution of the solution of the 1D Allen-Cahn equation shown in Figure 4(b). For example, within the interval $[-0.5, 0]$, the output of the plain network first goes down significantly and then goes up significantly towards the constant value 1, which is not the same as the evolution of the solution of the 1D Allen-Cahn equation. Moreover, when the training is converged, the relative L^2 error of this plain network is 0.08, which is much larger than the error 7.8×10^{-3} by using our EStable-Net.

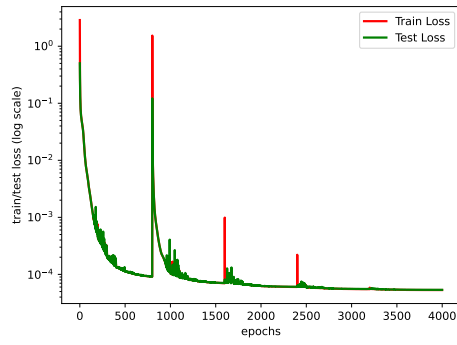
4.2 Allen-Cahn equation in two dimensions

In this subsection, we solve the Allen-Cahn equation in two dimension (2D). In this case, the spatial domain $\Omega = [-1, 1]^2$, and $\epsilon = 0.02$.

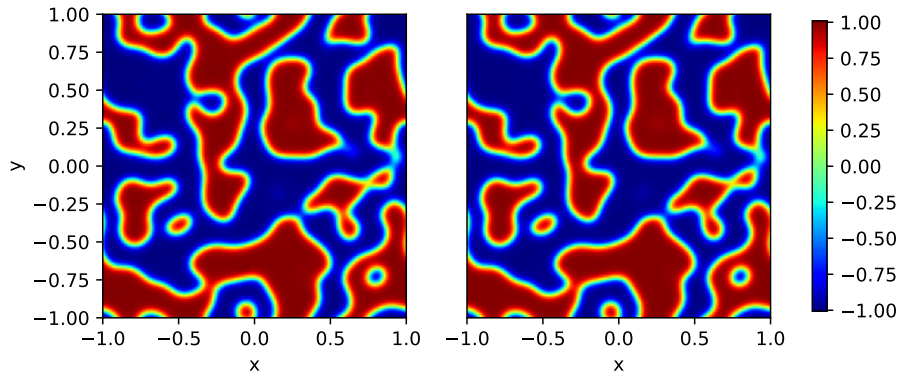
We choose $M = 5$ energy decay blocks in the network EStable-Net, and each block is composed of Conv2d-Tanh-Conv2d-Tanh, where Conv1d is a 2D convolution layer and Tanh is the activation using the tanh function. The activation function is not applied in the last layer for better accuracy. The number of channels is $1 - 16 - 1 - 16 - 1$ with kernel size 13. Under this setting, our EStable-Net has 54250 trainable parameters. We use the default (kaiming uniform) initialization for weights and the batch size is 32. The optimizer of our model is Adam [16] with initial learning rate 10^{-3} and L^2 regularization weight decay rate 10^{-7} . The learning rate decays by half every 100 epochs, and restarts for each 800 epochs.

The inputs ϕ_0 are generated by combing fourier basis function with frequency less than 8 and coefficients sampled from normal distribution. We use 128×128 evenly spaced grid points to discretize the spacial domain $[-1, 1]^2$. The label data $\phi(x, T)$ at $T = 5$ is calculated by pseudo-spectral method with the Fast Fourier Transform. For the time discretization, we adopt ode45 solver in MATLAB. We generate 2528 pairs of data $\phi(x, 0)$ and $\phi(x, 5)$, and 2048 of them are used for training while the left 480 are used for testing.

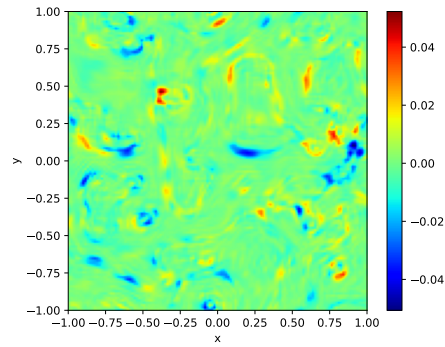
Results of accuracy of EStable-Net on this 2D Allen Cahn equation are shown in Figure 5. After 4000 epochs of training, the test loss reaches about 5.3×10^{-5} and the



(a) Train/test loss (MSE)



(b) Predicted (left) v.s. reference solution (right)

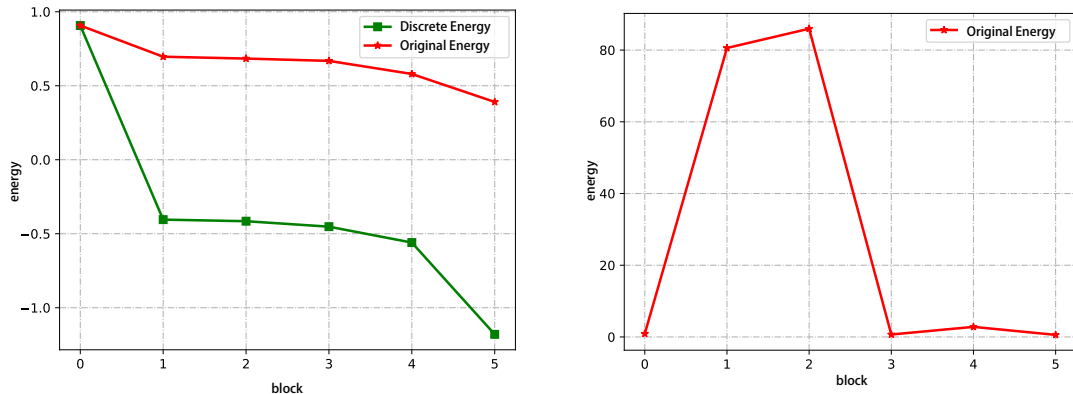


(c) Absolute error of the prediction in (b)

Figure 5: 2D Allen-Cahn equation: EStable-Net accuracy

relative L^2 error reaches 8.8×10^{-3} , as shown in Figure 5(a). Figure 5(b) and (c) show an example that the prediction of our network agrees well with the exact solution.

By randomly selecting 256 examples and passing them into the trained EStable-Net, we output the discrete energy in Eq. (26) after each block. As in the 1D case reported above, we find that in all the samples of the 2D case, the discrete energy is decreasing block by block, as predicted by analysis. Moreover, we also find that the original energy in Eq. (3) is also decreasing block by block. These results of energies are shown in Figure 6(a).



(a) Energies after each block in EStable-Net (b) Energy after each block in a plain network without the energy stable design

Figure 6: 2D Allen-Cahn equation: energy comparisons

The output of the intermediate and final blocks in EStable-Net and the corresponding snapshots in the evolution of the solution of the 2D Allen-Cahn equation with equal time increment $T/5$ obtained by numerical method are shown in Figures 7 and 8, respectively. It can be seen that the evolution trend of the output of the intermediate blocks in ECDnet is consistent with the evolution of the solution of the 2D Allen-Cahn equation.

We also compare the evolving of the energy with that by using a "plain" network based on these selected samples; see Figure 6(b). The "plain" network does not have the auxiliary variable U and the associated energy stable property as described in the 1D case in the previous subsection. It can be seen that the energy (which is given by Eq. (3)) increases significantly at the first two blocks and then decreases at the third block as shown in Figure 6(b), which is not consistent with the property of the gradient flow. The output of the intermediate and final blocks in this plain network

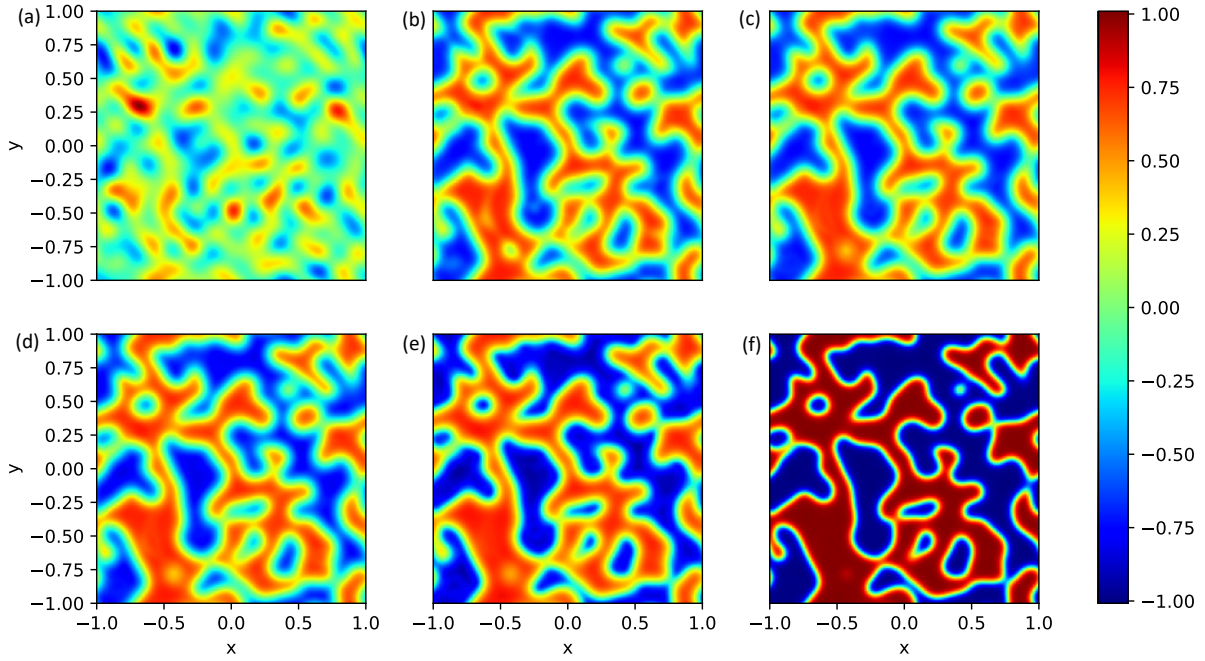


Figure 7: 2D Allen-Cahn equation: initial state and output of intermediate and final blocks in EStable-Net from (a) to (f).

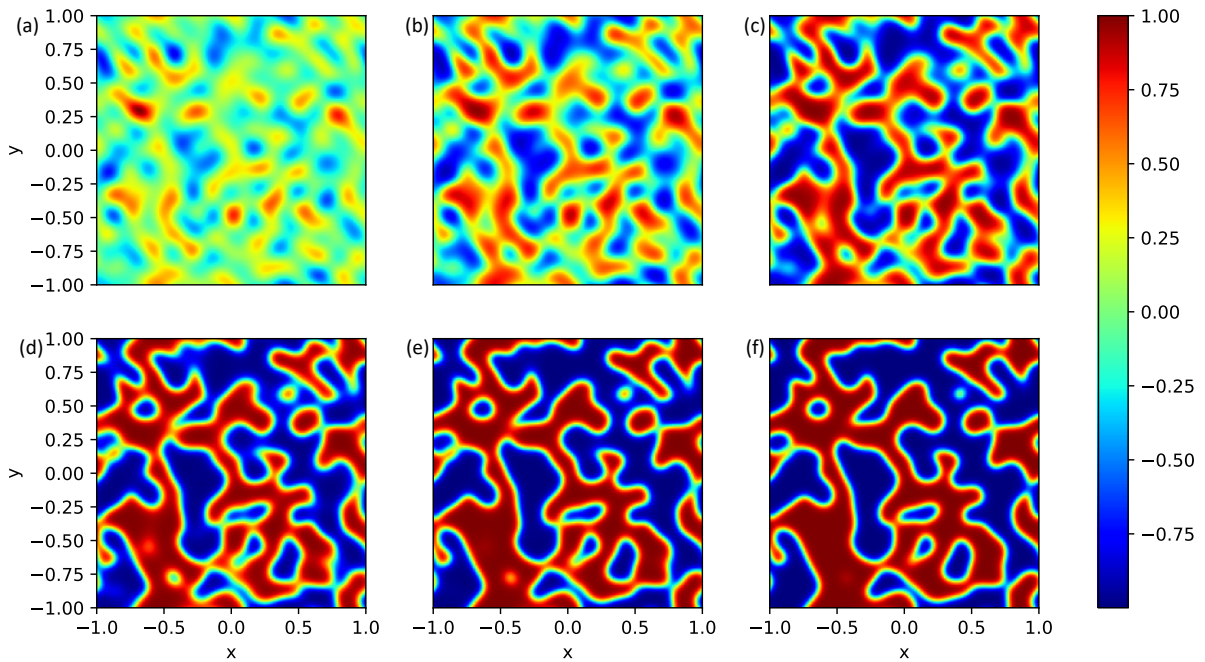


Figure 8: 2D Allen-Cahn equation: snapshots in the evolution of the 2D Allen-Cahn equation with time interval $T/5$ obtained by numerical method.

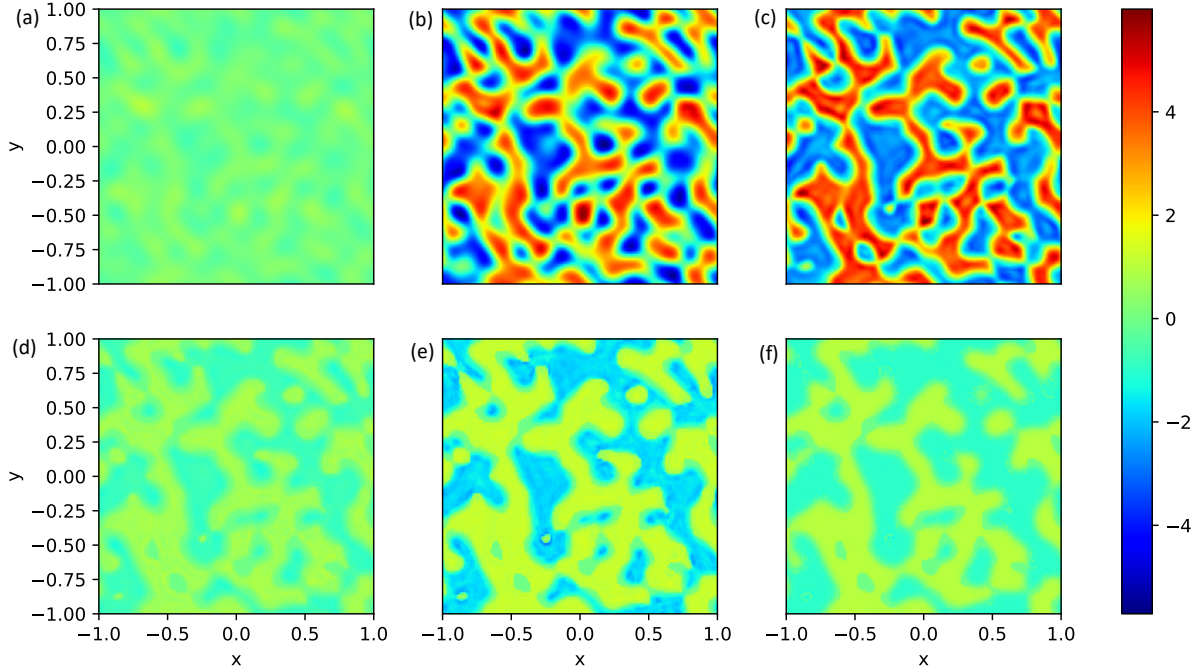


Figure 9: 2D Allen-Cahn equation: initial state and output of intermediate and final blocks in the plain network from (a) to (f).

are shown in Figure 9. It can be seen that the intermediate states given by this plain network are not consistent with the evolution of the solution of the 2D Allen-Cahn equation shown in Figure 8. Moreover, when the training is converged, the relative L^2 error of this plain network is 0.22, which is much larger than the error 8.8×10^{-3} by using our EStable-Net.

5 Conclusions

In this paper, we propose an energy stable neural network (EStable-Net) for solving gradient flow equations. We first rewrite the gradient flow equation into an equivalent form by introducing an auxiliary variable. The solution update scheme in our neural network EStable-Net is inspired by this auxiliary variable based equivalent form of the gradient flow equation, and enables decreasing of a discrete energy along the neural network.

The architecture of the neural network EStable-Net consists of a few energy decay

blocks, and the output of each block can be interpreted as an intermediate state of the evolution process of the gradient flow equation, following the Autoflow structure in the neural network DOSnet [18]. This design of identical input and output dimensions in the intermediate blocks vastly reduces the parameters of the neural network. We prove that an discrete energy calculated after each block is decreasing along the network, which is consistent with the property in the evolution process of the gradient flow equation. The proposed EStable-Net can be applied generally to a wide range of gradient flow equations.

We perform numerical experiments of the EStable-Net on the Allen-Cahn equation in one and two dimensions. The numerical experimental results demonstrate that our network is able to generate high accuracy and stable predictions.

Acknowledgments

The work of Yang Xiang was supported in part by HKUST IEG19SC04 and the Project of Hetao Shenzhen-HKUST Innovation Cooperation Zone HZQB-KCZYB-2020083.

References

- [1] Fan Chen, Jianguo Huang, Chunmei Wang, and Haizhao Yang. Friedrichs learning: Weak solutions of partial differential equations via deep learning. *SIAM Journal on Scientific Computing*, 45(3):A1271–A1299, 2023.
- [2] Jingrun Chen, Xurong Chi, Weinan E, and Zhouwang Yang. Bridging traditional and machine learning-based algorithms for solving PDEs: The random feature method. *Journal of Machine Learning*, 1(3):268–298, 2022.
- [3] Wenbin Chen, Sidafa Conde, Cheng Wang, Xiaoming Wang, and Steven M Wise. A linear energy stable scheme for a thin film model without slope selection. *Journal of Scientific Computing*, 52(3):546–562, 2012.

- [4] Yuyan Chen, Bin Dong, and Jinchao Xu. Meta-MgNet: Meta multigrid networks for solving parameterized partial differential equations. *Journal of Computational Physics*, 455:110996, 2022.
- [5] M.W.M.G. Dissanayake and N. Phan-Thien. Neural-network-based approximations for solving partial differential equations. *Communications in Numerical Methods in Engineering*, 10(3):195–201, 1994.
- [6] Weinan E. A proposal on machine learning via dynamical systems. *Communications in Mathematics and Statistics*, 1(5):1–11, 2017.
- [7] Weinan E and Bing Yu. The deep ritz method: a deep learning-based numerical algorithm for solving variational problems. *Communications in Mathematics and Statistics*, 6(1):1–12, 2018.
- [8] C.M. Elliott and A.M. Stuart. The global dynamics of discrete semilinear parabolic equations. *SIAM J. Numer. Anal.*, 30:1622–1663, 1993.
- [9] D.J. Eyre. Unconditionally gradient stable time marching the Cahn–Hilliard equation. In *Computational and Mathematical Models of Microstructural Evolution, Mater. Res. Soc. Symp. Proc., vol. 529*, pages 39–46. MRS, Warrendale, PA, 1998.
- [10] Yuwei Fan and Lexing Ying. Solving electrical impedance tomography with deep learning. *Journal of Computational Physics*, 404:109119, 2020.
- [11] Craig R. Gin, Daniel E. Shea, Steven L. Brunton, and J. Nathan Kutz. Deep-Green: Deep learning of Green’s functions for nonlinear boundary value problems. *Scientific Reports*, 11:21614, 2021.
- [12] I. Goodfellow, Y. Bengio, and A. Courville. *Deep Learning*. MIT Press, Cambridge, MA, 2016.
- [13] F. Guillén-González and G. Tierra. On linear schemes for a Cahn–Hilliard diffuse interface model. *J. Comput. Phys.*, 234:140–171, 2013.
- [14] Jiequn Han, Arnulf Jentzen, and Weinan E. Solving high-dimensional partial differential equations using deep learning. *Proceedings of the National Academy of Sciences*, 115(34):8505–8510, 2018.
- [15] Yuehaw Khoo, Jianfeng Lu, and Lexing Ying. Solving parametric PDE problems with artificial neural networks. *European Journal of Applied Mathematics*, 32(3):421–435, 2021.

- [16] Diederik P Kingma and Jimmy Ba. Adam: A method for stochastic optimization. *arXiv preprint arXiv:1412.6980*, 2014.
- [17] Isaac E. Lagaris, Aristidis Likas, and Dimitrios I. Fotiadis. Artificial neural networks for solving ordinary and partial differential equations. *IEEE Transactions on Neural Networks*, 9(5):987–1000, 1998.
- [18] Yuan Lan, Zhen Li, Jie Sun, and Yang Xiang. Dosnet as a non-black-box pde solver: When deep learning meets operator splitting. *Journal of Computational Physics*, page 112343, 2023.
- [19] Y. LeCun, Y. Bengio Y, and G. Hinton. Deep learning. *Nature*, 521:436—444, 2015.
- [20] Zongyi Li, Nikola Kovachki, Kamyar Azizzadenesheli, Burigede Liu, Kaushik Bhattacharya, Andrew Stuart, and Anima Anandkumar. Fourier neural operator for parametric partial differential equations. *arXiv preprint arXiv:2010.08895*, 2020.
- [21] Lizuo Liu and Wei Cai. DeepPropNet – A recursive deep propagator neural network for learning evolution PDE operators. *arXiv preprint arXiv:2202.13429*, 2022.
- [22] Lu Lu, Pengzhan Jin, Guofei Pang, Zhongqiang Zhang, and George Em Karniadakis. Learning nonlinear operators via DeepONet based on the universal approximation theorem of operators. *Nature Machine Intelligence*, 3(3):218–229, 2021.
- [23] Liyao Lyu, Zhen Zhang, Minxin Chen, and Jingrun Chen. Mim: A deep mixed residual method for solving high-order partial differential equations. *Journal of Computational Physics*, 452:110930, 2022.
- [24] Qing Pan, Chong Chen, Yongjie Jessica Zhang, and Xiaofeng Yang. A novel hybrid IGA-EIEQ numerical method for the Allen–Cahn/Cahn–Hilliard equations on complex curved surfaces. *Computer Methods in Applied Mechanics and Engineering*, 404:115767, 2023.
- [25] Maziar Raissi, Paris Perdikaris, and George E Karniadakis. Physics-informed neural networks: A deep learning framework for solving forward and inverse problems involving nonlinear partial differential equations. *Journal of Computational physics*, 378:686–707, 2019.

- [26] Jie Shen, Cheng Wang, Xiaoming Wang, and Steven M Wise. Second-order convex splitting schemes for gradient flows with Ehrlich–Schwoebel type energy: application to thin film epitaxy. *SIAM Journal on Numerical Analysis*, 50(1):105–125, 2012.
- [27] Jie Shen, Jie Xu, and Jiang Yang. The scalar auxiliary variable (SAV) approach for gradient flows. *Journal of Computational Physics*, 353:407–416, 2018.
- [28] Jie Shen and Xiaofeng Yang. Numerical approximations of Allen–Cahn and Cahn–Hilliard equations. *Discrete Contin. Dyn. Syst*, 28(4):1669–1691, 2010.
- [29] Justin Sirignano and Konstantinos Spiliopoulos. DGM: A deep learning algorithm for solving partial differential equations. *Journal of Computational Physics*, 375:1339–1364, 2018.
- [30] Cheng Wang, Xiaoming Wang, and Steven M Wise. Unconditionally stable schemes for equations of thin film epitaxy. *Discrete and Continuous Dynamical Systems*, 28(1):405–423, 2010.
- [31] Steven M Wise, Cheng Wang, and John S Lowengrub. An energy-stable and convergent finite-difference scheme for the phase field crystal equation. *SIAM Journal on Numerical Analysis*, 47(3):2269–2288, 2009.
- [32] Xiaofeng Yang. Linear, first and second-order, unconditionally energy stable numerical schemes for the phase field model of homopolymer blends. *Journal of Computational Physics*, 327:294–316, 2016.
- [33] Xiaofeng Yang, Jia Zhao, Qi Wang, and Jie Shen. Numerical approximations for a three-component Cahn–Hilliard phase-field model based on the invariant energy quadratization method. *Mathematical Models and Methods in Applied Sciences*, 27(11):1993–2030, 2017.
- [34] Yahong Yang and Yang Xiang. Approximation of functionals by neural network without curse of dimensionality. *Journal of Machine Learning*, 1(4):342–372, 2022.
- [35] Yaohua Zang, Gang Bao, Xiaojing Ye, and Haomin Zhou. Weak adversarial networks for high-dimensional partial differential equations. *Journal of Computational Physics*, 411:109409, 2020.

- [36] Lulu Zhang, Tao Luo, Yaoyu Zhang, Weinan E, Zhi-Qin John Xu, and Zheng Ma. MOD-Net: A machine learning approach via model-operator-data network for solving PDEs. *Commun. Comput. Phys.*, 32:299–335, 2022.
- [37] J. Zhu, L. Chen, J. Shen, and V. Tikare. Coarsening kinetics from a variable mobility Cahn–Hilliard equation – application of semi-implicit fourier spectral method. *Phys. Rev. E*, 60:3564–3572, 1999.